

## Order and Disorder in Solids

### W4.1 Further Discussion of the Random Close-Packing Model

That the *random close-packing model* (RCP) is a more appropriate microscopic structural model for metallic glasses than, for example, a nanocrystalline model can be demonstrated using the results of diffraction studies of metallic glasses. To illustrate the differences between diffraction from amorphous and crystalline materials, the transmission electron-diffraction patterns of thin films of amorphous and recrystallized microcrystalline Fe are shown in Fig. W4.1. These two diffraction patterns can be seen to be qualitatively different, with microcrystalline Fe showing sharp diffraction rings and amorphous Fe showing instead only a few broad, diffuse diffraction rings.

The next-NN atomic configurations which are responsible for the second peak in the reduced radial distribution function  $G(r)$  for the metallic glass  $\text{Ni}_{0.76}\text{P}_{0.24}$ , shown in Fig. 4.11 of the textbook<sup>†</sup> are shown schematically in Fig. W4.2 for a planar, hexagonal array of close-packed atoms. It should be noted that in the RCP model such an array would not actually be planar, and the corresponding distances would be somewhat less than  $\sqrt{3}$  and 2. These distances are actually close to those expected in icosahedra (see Fig. 1.11). The overlapping structure of this second peak is thus a characteristic signature of metallic glasses with an RCP structure and may be considered to provide indirect evidence for the existence of icosahedral clusters of atoms in metallic glasses.

The fact that the RCP structural model is successful in predicting that two distinct types of atomic configurations contribute to the second peak in the radial distribution function  $g(r)$  provides strong evidence for its validity. In contrast, nanocrystalline models of metallic glasses are unable to explain the details of the observed  $g(r)$ . These models, based on the existence of nanocrystallites in the metallic glass, are able to predict the sharpness of the first peak. They predict, however, that the second and higher peaks will be sharper than actually observed. Thus the intermediate-range order predicted to extend beyond NN atoms by nanocrystalline models is not generally observed in amorphous solids.

One final observation concerning the RCP model is that it can be said to represent an “ideal” close-packed amorphous solid. This observation follows from the fact that in the RCP model the spheres are packed as densely as possible, consistent with the nature of amorphous solids. Achieving a higher density of packing of hard spheres would

<sup>†</sup>The material on this home page is supplemental to *The Physics and Chemistry of Materials* by Joel I. Gersten and Frederick W. Smith. Cross-references to material herein are prefixed by a “W”; cross-references to material in the textbook appear without the “W.”

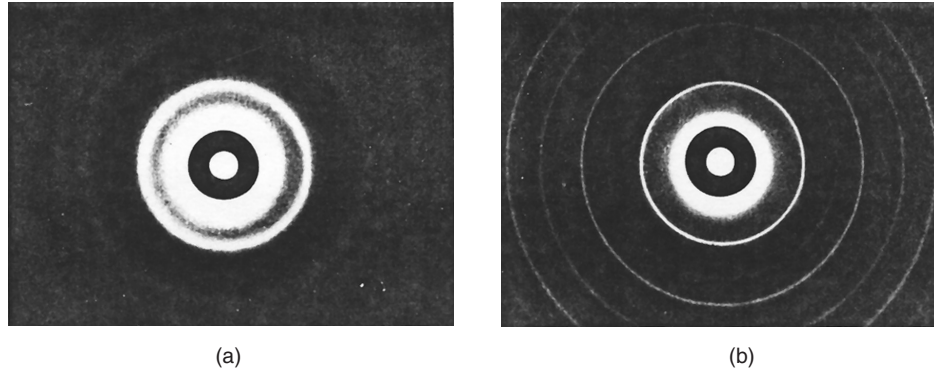


**Figure W4.1.** Transmission electron-diffraction patterns for thin films of (a) amorphous and (b) recrystallized microcrystalline Fe. (From T. Ichikawa, *Phys. Stat. Solidi a*, 19, 707 (1973). Reprinted by permission of Wiley-VCH Verlag Berlin.)

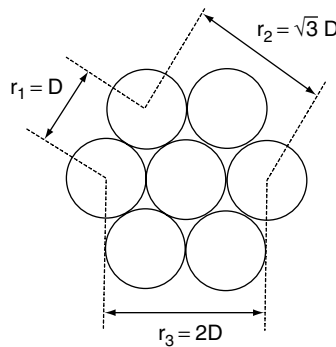


**Figure W4.2.** NN and two types of next-NN configurations of atoms in metallic glasses. A planar, hexagonal array of close-packed atoms is shown.

require that a form of crystallization occur locally, corresponding to the nucleation of clusters of spheres with either the FCC or HCP crystal structures or as icosahedra. The resulting solid would then, however, no longer be completely amorphous. A lower density of packing could easily be achieved by removing spheres, thereby creating vacancies and causing the resulting structure to be even more disordered than the ideal amorphous solid represented by the RCP model.

Even though it can be argued that the RCP model is in some sense ideal, it nevertheless defines an amorphous structure only in a statistical way. This follows from the fact that there can be an infinite number of possible amorphous solids with structures that are consistent with the RCP structural model, whereas a crystalline solid has a single, unique structure.

#### W4.2 Further Discussion of the Continuous Random Network Model

In the case of amorphous carbon, a-C, there is little doubt that a *continuous random network model* (CRN) is appropriate, but there is great difficulty in knowing how to

construct such a model. The difficulty resides in the fact that there are two common forms of crystalline C: graphite, based on C–C<sub>3</sub> trigonal bonding units, and diamond, based on C–C<sub>4</sub> tetrahedral bonding units. Both graphitelike and diamondlike types of SRO are believed to be present in a-C.

The validity of CRN models for amorphous solids such as a-Si, a-SiO<sub>2</sub>, and a-Ge has been verified by comparing the experimentally determined radial distribution functions with those calculated from “ball-and-stick” CRN models constructed by hand and “relaxed” by computer to minimize network strain. The agreement between experiment and the predictions of the CRN models has been found to be impressive.<sup>†</sup> These comparisons also demonstrate that nanocrystalline models for amorphous covalent (or nearly covalent) glasses are inappropriate, as was also found to be the case for metallic glasses.

### W4.3 Illustrations of the Law of Mass Action

For Schottky defects (i.e., vacancies) the process of creating a vacancy  $V_A$  without a corresponding interstitial  $I_A$  involves the movement of an A atom from a lattice site to a surface site (i.e.,  $S_A$ ). The defect reaction for this process is



At the same time, an existing surface atom  $S_A$  is covered. The net effect is that an additional bulk atom is created below the surface, yielding



The net defect reaction is therefore the sum of reactions (W4.1) and (W4.2); that is,



The law of mass action for the creation of a Schottky defect is therefore

$$a_L(V) = \frac{N_L(V)}{N_L(A)} = K_V(T), \quad (\text{W4.4})$$

which yields

$$N_L(V) = N_L(A) \exp\left(-\frac{\Delta G_r}{k_B T}\right). \quad (\text{W4.5})$$

The process of creating an interstitial without a corresponding lattice vacancy involves the movement of a surface atom  $S_A$  into an empty interstitial position  $V_I$ , thus creating an interstitial A atom  $I_A$ . At the same time, a new surface atom is uncovered. The resulting interstitial number or concentration is given by

$$N_I(A) = N_I(V) \exp\left(-\frac{\Delta G_r}{k_B T}\right). \quad (\text{W4.6})$$

<sup>†</sup> An excellent summary of these comparisons appears in Zallen (1983, Chap. 2).

When taken together, the processes just described for the creation of a Schottky defect and of an interstitial atom are equivalent to the creation of a Frenkel defect (i.e., a vacancy–interstitial pair). It can be shown that the equilibrium constant for Frenkel defect formation  $K_F$  is equal to  $K_V K_I$  (i.e., to the product of the equilibrium constants  $K_V$  for vacancy formation and  $K_I$  for interstitial formation).

The generation of charged defects (i.e., ionized donors and acceptors in semiconductors) is described in detail in Chapter 11. The requirement of electrical neutrality plays an important role in determining the concentrations of ionized dopant atoms and, consequently, of charge carriers.

#### W4.4 Nonstoichiometry

Solids such as  $\text{SiO}_2$ ,  $\text{NaCl}$ ,  $\text{V}_3\text{Si}$ , and  $\text{YBa}_2\text{Cu}_3\text{O}_7$ , which have a well-defined chemical formula are stoichiometric compounds. When the composition of a solid deviates from the standard chemical formula, the resulting solid is said to be *nonstoichiometric*, and as a result, defects are present. Examples include  $\text{SiO}_{2-x}$ ,  $\text{Fe}_3\text{O}_{4-x}$ ,  $\text{YBa}_2\text{Cu}_3\text{O}_{7-x}$ , and  $\text{Mn}_{1-x}\text{O}$ . Additional examples of nonstoichiometric solids are discussed in Chapter 4, with further examples presented in Chapters 11 to 18, where specific classes of materials are addressed.

Nonstoichiometry often results when a solid comes into equilibrium with external phases. For example, the first three solids just listed are all oxygen-deficient, possibly resulting from being in equilibrium with an oxygen-deficient atmosphere either during growth or during subsequent processing at elevated temperatures. The fourth example,  $\text{Mn}_{1-x}\text{O}$ , is likely to have been formed in an oxygen-rich atmosphere. In all four cases, the actual composition of the solid is determined by the oxygen activity of the ambient (i.e., the partial pressure of  $\text{O}_2$ ), by the temperature, and by the chemical potentials of the components.

Nonstoichiometry and the existence of point defects in a solid are often closely related. Anion vacancies are the source of the nonstoichiometry in  $\text{SiO}_{2-x}$ ,  $\text{Fe}_3\text{O}_{4-x}$ , and  $\text{YBa}_2\text{Cu}_3\text{O}_{7-x}$ , and cation vacancies are present in  $\text{Mn}_{1-x}\text{O}$ . In some cases the vacancies within the structure are ordered. Nonstoichiometry in ionic solids usually corresponds to at least one of the ions occurring in more than one charge state. For example, if all the oxygen ions in  $\text{Mn}_{1-x}\text{O}$  are  $\text{O}^{2-}$ , then for every  $\text{Mn}^{2+}$  vacancy in the solid there must also be two  $\text{Mn}^{3+}$  ions present to preserve overall electrical neutrality.

#### REFERENCE

Zallen, R., *The Physics of Amorphous Solids*, Wiley, New York, 1983.